Regulation of *miR399f* Transcription by AtMYB2 Affects Phosphate Starvation Responses in Arabidopsis[1][W]

Dongwon Baek[2], Min Chul Kim[2], Hyun Jin Chun[2], Songhwa Kang, Hyeong Cheol Park, Gilok Shin, Jiyoung Park, Mingzhe Shen, Hyewon Hong, Woe-Yeon Kim, Doh Hoon Kim, Sang Yeol Lee, Ray A. Bressan, Hans J. Bohnert, and Dae-Jin Yun*

Division of Applied Life Science (BK21 Program), Plant Molecular Biology and Biotechnology Research Center, Gyeongsang National University, Jinju 660–701, Korea (D.B., M.C.K., H.J.C., S.K., H.C.P., G.S., J.P., M.S., H.H., W.-Y.K., S.Y.L., D.-J.Y.); College of Life Science and Natural Resources, Dong-A University, Busan 604–714, Korea (D.H.K.); Department of Horticulture and Landscape Architecture, Purdue University, West Lafayette, Indiana 47907 (R.A.B.); Department of Plant Biology and Department of Crop Sciences, University of Illinois at Urbana-Champaign, Urbana, Illinois 61801 (H.J.B.); and College of Science, King Abdulaziz University, Jeddah 21589, Saudi Arabia (R.A.B., H.J.B.)

Although a role for *microRNA399* (*miR399*) in plant responses to phosphate (Pi) starvation has been indicated, the regulatory mechanism underlying *miR399* gene expression is not clear. Here, we report that *AtMYB2* functions as a direct transcriptional activator for *miR399* in Arabidopsis (*Arabidopsis thaliana*) Pi starvation signaling. Compared with untransformed control plants, transgenic plants constitutively overexpressing *AtMYB2* showed increased *miR399f* expression and tissue Pi contents under high Pi growth and exhibited elevated expression of a subset of Pi starvation-induced genes. Pi starvation-induced root architectural changes were more exaggerated in *AtMYB2*-overexpressing transgenic plants compared with the wild type. AtMYB2 directly binds to a MYB-binding site in the *miR399f* promoter in vitro, as well as in vivo, and stimulates *miR399f* promoter activity in Arabidopsis protoplasts. Transcription of *AtMYB2* itself is induced in response to Pi deficiency, and the tissue expression patterns of *miR399f* and *AtMYB2* are similar. Both genes are expressed mainly in vascular tissues of cotyledons and in roots. Our results suggest that *AtMYB2* regulates plant responses to Pi starvation by regulating the expression of the *miR399* gene.

Phosphorus (P) is an essential component of all organisms, as it is found, among other compounds, in nucleic acids, ATP, and membrane phospholipids. It is an essential nutrient for plants. P can be acquired by plants only as inorganic phosphate (Pi). Therefore, most of the P content of soils is unavailable for plant growth and development (Hinsinger, 2001). To overcome the problem of Pi limitation, plants have developed a variety of adaptive responses that conserve internal P while activating mechanisms that enhance the accessibility and uptake of external P. The accompanying gene expression changes produce changes in root architecture, enhanced Pi uptake activity, secretion of organic acids, and secretion of phosphatases (Raghothama, 1999; Poirier and Bucher, 2002; Yuan and Liu, 2008; Péret et al., 2011). The synchronization of Pi availability with plant growth and development is orchestrated by several phytohormones, including abscisic acid, ethylene, auxin, and cytokinin (Hillwig et al., 2008; Devaiah et al., 2009; Lei et al., 2011).

A few transcription factors have been characterized that appear to regulate subsets of the response to Pi stress, either positively or negatively. PHOSPHATE STARVATION RESPONSE1 (PHR1) is a MYB transcription factor that initiates the up-regulation of Pi starvation-responsive genes in plants and unicellular algae (Rubio et al., 2001). WRKY75, a WRKY transcription factor family member, has been identified as a key regulator of Pi acquisition and root architecture in response to Pi starvation (Devaiah et al., 2007a). MYB62, an R2R3-type MYB transcription factor, connects Pi homeostasis and GA signaling during Pi starvation (Devaiah et al., 2009). ZAT6, a C2H2-type zinc finger transcription factor, regulates Pi homeostasis and exerts some control over root development (Devaiah et al., 2007b). The BHLH32 (for basic helix-loop-helix) transcription factor is a negative regulator of several Pi starvation responses (Chen et al., 2007). *PTF1*, of rice (*Oryza sativa*) and maize (*Zea mays*), encodes a bHLH transcription factor that is involved in Pi signaling (Yi et al., 2005; Li et al., 2011). These transcription factors function in cross talk between Pi

[1] This work was supported by the World Class University Program funded by the Ministry of Education, Science, and Technology (grant no. R32–10148), Republic of Korea, and by the Next-Generation BioGreen21 Program of the Rural Development Administration (grant no. PJ008025), Republic of Korea.

[2] These authors contributed equally to the article.

* Corresponding author; e-mail djyun@gnu.ac.kr.

The author responsible for distribution of materials integral to the findings presented in this article in accordance with the policy described in the Instructions for Authors (www.plantphysiol.org) is: Dae-Jin Yun (djyun@gnu.ac.kr).

[W] The online version of this article contains Web-only data.

www.plantphysiol.org/cgi/doi/10.1104/pp.112.205922

starvation signaling and signaling by phytohormones, or photosynthates, to govern physiological responses to Pi limitation (Rouached et al., 2010).

MicroRNAs (miRNAs) are endogenous noncoding RNAs, 21 to 24 nucleotides in length, that contribute to the regulation of gene expression. They have emerged as master regulators in plant development, and they orchestrate adaptive responses to stresses owing to posttranscriptional regulation of gene expression (Bonnet et al., 2006; Mallory and Vaucheret, 2006; Sunkar et al., 2012). Recently, the regulation of phosphate, copper, and sulfate homeostasis in plants was found to involve miRNAs (Jones-Rhoades and Bartel, 2004; Fujii et al., 2005; Chiou et al., 2006; Yamasaki et al., 2007; Liang et al., 2010; Kuo and Chiou, 2011). Pi deprivation induces the expression of several miRNAs in Arabidopsis (*Arabidopsis thaliana*), including *miR156*, *miR399*, *miR778*, *miR827*, and *miR2111* (Fujii et al., 2005; Hsieh et al., 2009; Pant et al., 2009). Of these, *miR2111* up-regulates the expression of *At3g27150*, which encodes a Kelch repeat-containing F-box protein (Hsieh et al., 2009). *miR827* mediates cross talk between Pi and nitrogen limitation signaling, based on the regulation of anthocyanin synthesis. It also down-regulates the expression of *At1g02860* that encodes a ubiquitin E3 ligase (Hsieh et al., 2009; Pant et al., 2009). Irrespectively, the precise role of these Pi limitation-induced miRNAs in the regulation of Pi homeostasis remains unknown (Doerner, 2008; Kuo and Chiou, 2011).

In contrast, the mode of action for *miR399* during plant responses to Pi starvation is well characterized. Expression of *miR399* is strongly induced upon Pi starvation, especially in vascular tissues of the shoot. Mature *miR399* is then translocated to roots and binds to the 5′ untranslated region of *PHO2* (*UBC24*, which encodes a ubiquitin-conjugating E2 enzyme) transcripts, leading to the degradation of *PHO2* mRNA. The resulting decrease of PHO2 protein level activates the expression of phosphate transporter genes, such as *Pht1;8* and *Pht1;9*, thereby facilitating Pi uptake and transport to the shoot (Fujii et al., 2005; Aung et al., 2006; Bari et al., 2006; Chiou et al., 2006; Pant et al., 2009). Thus, induction of *miR399* gene expression by Pi limitation plays an important role as the trigger in the restoration of Pi homeostasis by promoting Pi acquisition in roots and Pi allocation to shoots. Missing are mechanistic details of the

A

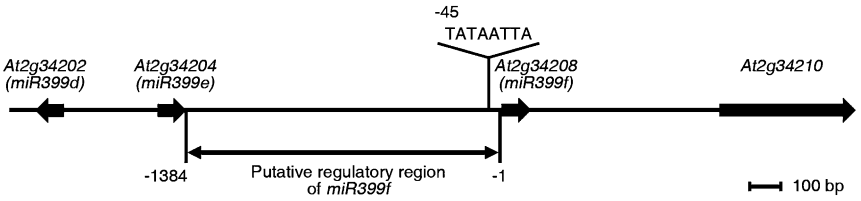

B

Putative *cis*-acting elements in *miR399f* promoter

Stresses	Site Name	Organism[a]	Position[b]	Strand[c]	Sequence
Abiotic Stress	MBS	*Arabidopsis thaliana*	-833	-	TAACTG
		Arabidopsis thaliana	-574	+	TAACTG
	PHR1-binding	*Arabidopsis thaliana*	-85	+	GAATATGC
	LTR	*Hordeum vulgare*	-1157	+	CCGAAA
Defense	ARE	*Zea mays*	-1041	+	TGGTTT
Jasmonic acid	TGACG-motif	*Hordeum vulgare*	-770	+	TGACG
	CGTCA-motif	*Hordeum vulgare*	-770	-	CGTCA
Light response	ACE	*Petroselinum crispum*	-896	+	AAAACGTTTA
	AT1-motif	*Solanum tuberosum*	-1067	+	ATTAATTTTACA
	GT1-motif	*Solanum tuberosum*	-1193	-	GTGTGTGAA
	CATT-motif	*Zea mays*	-1179	-	GCATTC
	GA-motif	*Arabidopsis thaliana*	-891	-	ATAGATAA
	GAG-motif	*Spinacia oleracea*	-941	-	AGAGATG
		Spinacia oleracea	-22	+	AGAGATG
	MRE	*Petroselinum crispum*	-1025	-	AACCTAA
		Petroselinum crispum	-735	+	AACCTAA
		Petroselinum crispum	-454	-	AACCTAA
	I-box	*Pisum sativum*	-892	-	TAGATAACC
	AE-box	*Arabidopsis thaliana*	-408	-	AGAAACAT
	Box 1	*Pisum sativum*	-740	+	TTTCAAA
	Box 4	*Petroselinum crispum*	-158	+	ATTAAT

[a] This is the species in which the *cis*-acting element sequence was first described.

[b] Positions are relative to the *miR399f* precursor start site.

[c] (+) and (-) indicate sense or antisense DNA strands.

Figure 1. Putative cis-acting regulatory elements in the *miR399f* promoter. A, Genomic organization of *miR399f* (*At2g34208*) flanking regions. The location of the TATA-like sequence (TATAATTA) of the *miR399f* gene is indicated. B, Putative cis-acting regulatory sequences on the *miR399* promoter. An area 1,384 bp upstream of the transcription start site was analyzed using PlantCARE. The selected matrix score for all cis-acting elements was 5 or greater. MBS, MYB2-binding site; LTR, low-temperature response; ARE, anaerobic response element; ACE, ACGT-containing element; MRE, MYB recognition element; AE-box, activating element box.

regulation of *miR399* gene expression in response to Pi starvation. In fact, information on the transcriptional regulation of miRNA genes is generally scarce, although much is known about the genomic organization of miRNA genes, molecular mechanisms of miRNA biogenesis, and miRNA functions in animals and plants (Jones-Rhoades et al., 2006).

We demonstrate here that the positive regulation of *miR399* gene expression in response to Pi starvation is mediated at least in part by the transcription factor AtMYB2. AtMYB2, a transcription factor that is known to function in abiotic stress signaling in Arabidopsis (Urao et al., 1996; Abe et al., 1997, 2003; Yoo et al., 2005), directly binds to a MYB-binding site located in the *miR399f* promoter. This enhances *miR399f* promoter activity. *AtMYB2* is coexpressed with *miR399f* in vascular tissue, and its transcript level is increased by Pi deprivation like that of *miR399f*. Constitutive overexpression (OE) of *AtMYB2* in Arabidopsis activates the transcription of *miR399f* and increases a subset of *PHOSPHATE STARVATION INDUCED* (*PSI*) gene expression, Pi uptake, and promotes changes in root architecture. These results uncover a missing link between Pi starvation and *miR399* transcription that also connects abiotic stress signaling to growth responses and Pi acquisition in the plant.

RESULTS

AtMYB2 Expression, Like *mi399f*, Is Induced by Phosphate Deficiency

The induction of *miR399f* gene expression in response to Pi deficit is the earliest known step in the signaling pathway leading from the sensing of Pi deficiency to changes in root architecture and the restoration of Pi homeostasis in Arabidopsis (Fujii et al., 2005; Hsieh et al., 2009). To uncover mechanisms involved in controlling *miR399f* gene expression, we performed an in silico analysis of its presumptive promoter region using the PlantCARE database (http://bioinformatics.psb.ugent.be/webtools/plantcare/html/; Fig. 1). Several cis-acting regulatory elements typically associated with biotic and abiotic stress responses, such as defense, jasmonic acid, and light signaling, were identified in this region. Also found were two canonical binding sites for AtMYB2, a drought-inducible transcription activator of the dehydration-responsive gene *RD22* that also participates in abscisic acid and salt stress signaling (Urao et al., 1996; Abe et al., 1997, 2003; Yoo et al., 2005). To test whether *AtMYB2* plays a role in *miR399f*-mediated Pi starvation signaling, we compared the expression of *AtMYB2* and the *miR399f* precursor transcript in wild-type seedlings after transfer from normal growth medium to high-Pi (1.25 mM KH_2PO_4), low-Pi (0.0125 mM KH_2PO_4), or Pi-deficient (0 mM KH_2PO_4) media by quantitative real-time (qRT)-PCR. The temporal expression pattern of *miR399f* precursor was similar to that of *AtMYB2* at all three Pi levels (Fig. 2). Significant increases in the steady-state levels of *AtMYB2* and *miR399f* transcripts were observed in shoots and roots after 5 and 7 d of exposure to low Pi or Pi deficiency. However, no increase in *AtMYB2* or *miR399f* transcript abundance was observed after exposure to high Pi. These results suggested that *AtMYB2* may be involved in *miR399f*-mediated Pi deficiency signaling in Arabidopsis.

miR399f and *AtMYB2* Are Expressed in the Same Plant Tissues

miR399 is expressed mainly in the vascular tissues of cotyledons, leaves, and roots. The expression in these tissues is strongly enhanced by Pi starvation

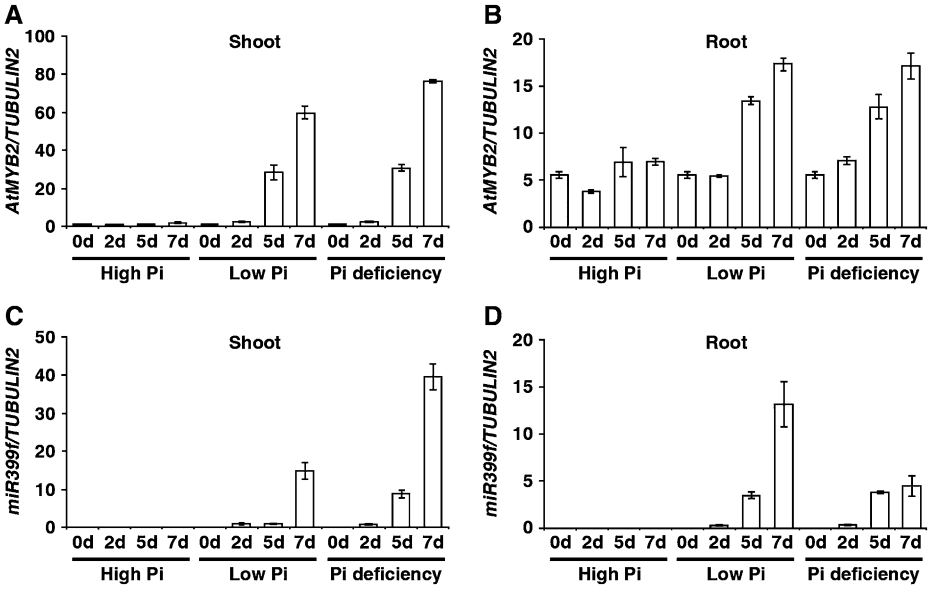

Figure 2. Expression of *AtMYB2* and the *miR399f* precursor is induced in response to phosphate deficit. A to D, Wild-type plants were grown on MS medium for 7 d, transferred to high-Pi, low-Pi, or Pi-deficient growth medium, and allowed to grow further for 0, 2, 5, and 7 d. Transcript levels were measured by qRT-PCR in total RNA extracted from shoots and roots at the indicated time points. Transcript levels of *AtMYB2* (A and B) and *miR399f* precursor (C and D), normalized to the transcript level of *TUBULIN2*, are shown. Bars represent means ± SD of three biological replicates with two technical replicates each.

(Aung et al., 2006). In order to investigate whether *AtMYB2* is expressed in the same plant organs and tissues, we performed histochemical analysis of *GUS* expression in tissues of *PromiR399f*:*GUS* and *ProAtMYB2*:*GUS* transgenic plants grown in high-Pi, low-Pi, and Pi-deficient medium (Fig. 3). As reported earlier (Aung et al., 2006), weak expression of the *miR399f* promoter was detected by GUS staining in the vascular tissues of cotyledons and leaves but not in roots of seedlings grown in high Pi (Fig. 3, A–D). Strong *miR399f* promoter activity was observed in vascular tissues of cotyledons, rosette leaves, and primary and lateral roots of seedlings grown under Pi deficit, but no activity was evident in root tips (Fig. 3, E–L). Under high-Pi, low-Pi, and Pi-deficient conditions, *GUS* activity was weaker in tissues of *ProAtMYB2*:*GUS* transgenic seedlings than in the corresponding tissues of *PromiR399f*:*GUS* seedlings. Consequently, only weak GUS staining was observed in vascular tissues of cotyledons in *ProAtMYB2*:*GUS* seedlings in high-Pi medium, and no GUS stain was observed in rosette leaves or primary and lateral roots (Fig. 3, M–P). Clear induction of *AtMYB2* promoter activity was observed in response to Pi limitation in cotyledons (Fig. 3, Q and U) and lateral roots (Fig. 3, T and X). Overall, the *GUS* reporter expression patterns in tissues of *ProAtMYB2*:*GUS* and *PromiR399f*:*GUS* seedlings were essentially similar, indicating that *AtMYB2* and *miR399f* are expressed in the same plant tissues, particularly under Pi limitation. These results suggest direct regulation of *miR399f* expression by AtMYB2.

Constitutive OE of *AtMYB2* Promotes *miR399f* Expression and Increases Tissue Pi Content

Next, we generated transgenic *CaMV35S*:*AtMYB2* plants and selected three lines (*AtMYB2* OE) that showed constitutive high-, middle-, and low-level OE of *AtMYB2* under normal growth conditions (Fig. 4A). RNA gel-blot analysis showed that *miR399f* mRNA abundance was significantly higher in the *AtMYB2* OE transgenic plants compared with wild-type plants grown under identical conditions (Fig. 4C). The level of *miR399f* accumulation was correlated positively with the level of *AtMYB2* expression (Fig. 4, A and C). Thus, OE of *AtMYB2* leads to a proportional increase *miR399f* expression, even in the presence of sufficient Pi.

Constitutive expression of *miR399* leads to degradation of the *UBC24* (*PHO2*) transcript and elevated Pi accumulation in Arabidopsis even under high Pi

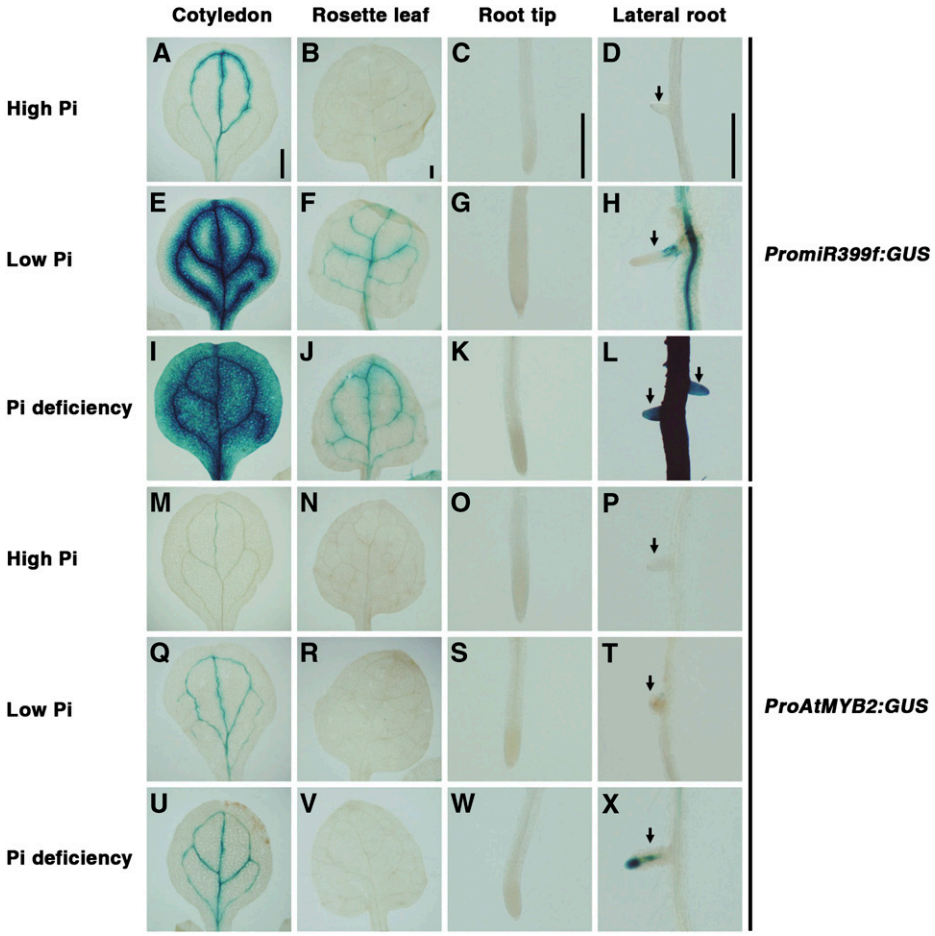

Figure 3. Spatial expression patterns of *miR399f* and *AtMYB2*. Seeds of *PromiR399f*:*GUS* and *ProAtMYB2*:*GUS* transgenic lines, which express the *GUS* reporter from the *miR399f* and *AtMYB2* promoters, respectively, were grown as described in Figure 5. Tissues were stained 7 d after transfer to high-Pi, low-Pi, or Pi-deficient medium. Blue color indicates GUS activity. A to L, Tissues of *PromiR399f*:*GUS* transgenic plants. M to X, Tissues of *ProAtMYB2*:*GUS* transgenic plants. Arrows indicate lateral roots. Bars = 0.5 mm.

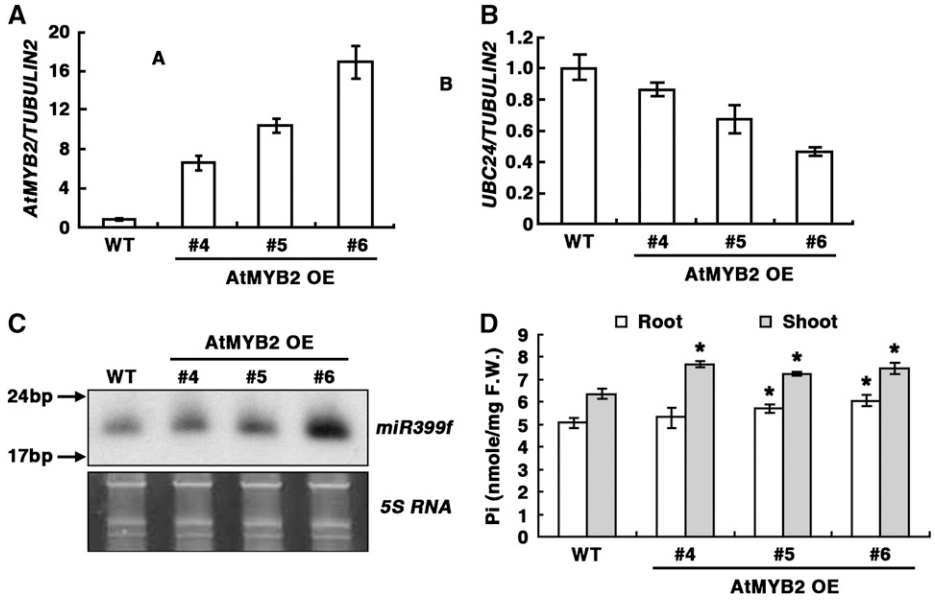

Figure 4. OE of *AtMYB2* induces *miR399f* expression and Pi accumulation. Wild type (WT) and three independent lines of *CaMV35S:AtMYB2* (AtMYB2 OE) were grown in MS medium. Ten-day-old seedlings were analyzed. A and B, Expression levels of *AtMYB2* (A) and *UBC24* (B), normalized to the level of *TUBULIN2*. Transcript levels were analyzed in total RNA extracted from the seedlings by qRT-PCR. Bars represent means ± SD for three biological replicates with two technical replicates each. C, Northern-blot analysis of *miR399f* expression in total RNA. Ethidium bromide-stained *5S rRNA* bands are shown as loading controls. D, Inorganic Pi concentrations were measured in the roots and shoots. Bars represent means ± SD for two biological replicates. Asterisks represent significant differences from the wild type ($P \leq 0.05$ from a Student's *t* test). F.W., Fresh weight.

(Fujii et al., 2005; Chiou et al., 2006). Accordingly, *AtMYB2* OE plants grown under high Pi accumulated lower levels of *UBC24* transcript than wild-type plants (Fig. 4B). A negative correlation was observed between mRNA levels of *UBC24* and *AtMYB2* or *miR399f* (Fig. 4, A–C). The Pi content in shoots of all three *AtMYB2* OE lines was significantly higher than that in wild-type plants (Fig. 4D), as predicted from their elevated *miR399f* expression levels and reduced *UBC2* expression levels on the basis of earlier reports (Fujii et al., 2005; Chiou et al., 2006). Elevated Pi accumulation was also observed in roots of the two *AtMYB2* OE lines that expressed the highest levels of *mi399f* transcript. Moreover, it has been reported that elevated Pi accumulation in *pho2* mutant and *miR399* OE Arabidopsis transgenic plants induced Pi toxicity-mediated chlorosis symptoms on their leaves (Fujii et al., 2005; Aung et al., 2006). To test whether *AtMYB2* OE plants also exhibit chlorosis symptoms, we grew wild-type and *AtMYB2* OE plants on Pi-sufficient Murashige and Skoog (MS) medium for 3 weeks under constant light conditions. We observed the development of typical chlorosis symptoms on the leaves of *AtMYB2* OE plants and also less chlorophyll content in *AtMYB2* OE plants compared with wild-type plants, supporting higher Pi content in *AtMYB2* OE plants than the wild type (Supplemental Fig. S1, A and B; Supplemental Materials and Methods S1). These results suggest that OE of *AtMYB2* affects Pi homeostasis in Arabidopsis by activating *miR399f*-mediated phosphate starvation signaling.

Pi Starvation-Induced Root Architectural Changes Are Exaggerated in *AtMYB2* OE Transgenic Plants

Under Pi limitation, root architecture is altered. Lateral root growth is promoted (increased lateral root number and length), while primary root length is reduced due to reduced cell elongation (Osmont et al., 2007; Desnos, 2008). Based on our results that OE of *AtMYB2* activated *miR399* accumulation and *miR399*-mediated Pi starvation signaling, we hypothesized that at least some Pi limitation-induced root architecture changes should be exaggerated in the *AtMYB2* OE lines. Accordingly, we investigated root morphology in wild-type plants, transgenic plants expressing empty vector, and *AtMYB2* OE transgenic plants 7 d after transfer from normal growth medium to high- and low-Pi media and to Pi-deficient medium (Fig. 5). Compared with plants grown in high-Pi medium, primary root lengths of wild-type and vector control seedlings grown in low-Pi and Pi-deficient media were lower by 20% to 30% (Fig. 5, A and B). However, low-Pi and Pi-deficient conditions resulted in a dramatic reduction (60%–70%) of primary root length of *AtMYB2* OE seedlings relative to growth in high Pi. Primary root lengths of *AtMYB2* OE seedlings were about 20% less than those of wild-type and

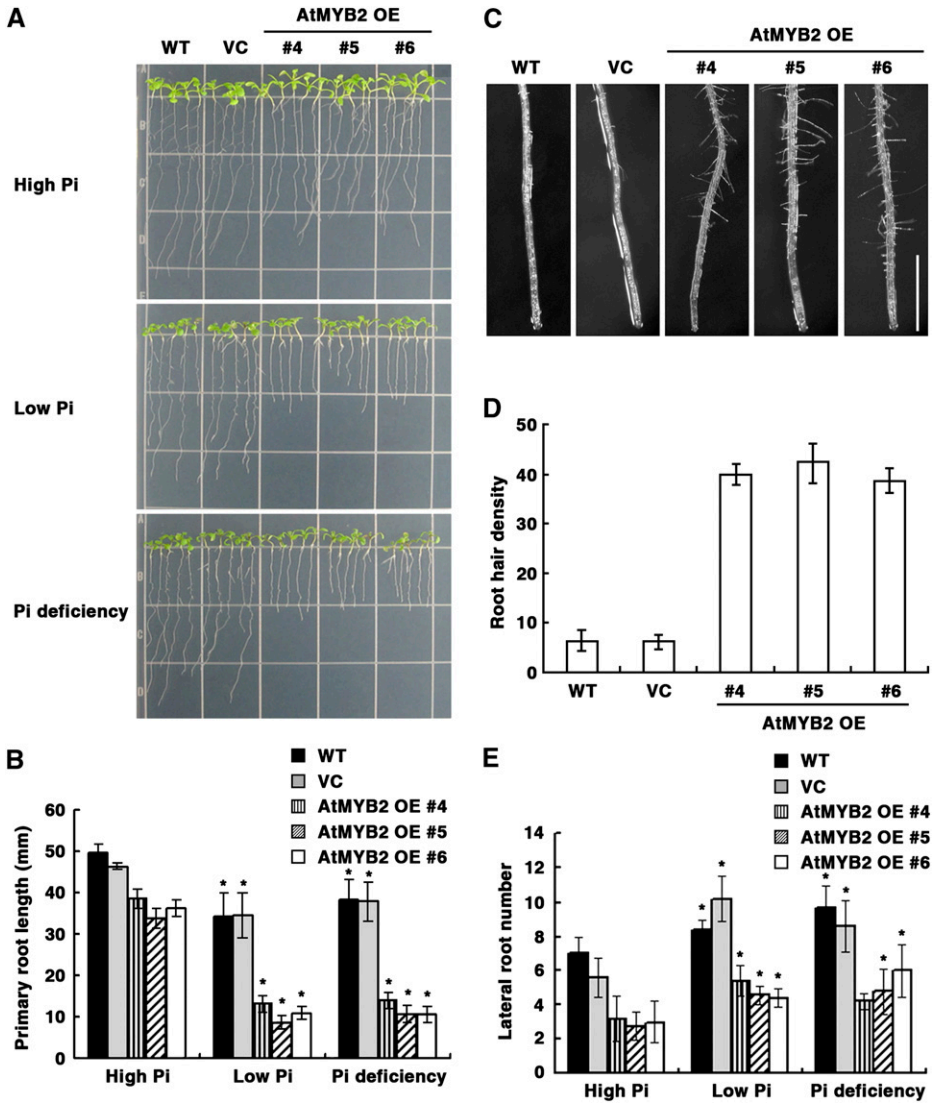

Figure 5. *AtMYB2* OE enhances Pi deficiency responses in root development and also affects root hair development. A, Seeds of the untransformed wild type (WT), empty vector control (VC) transformants, and three independent lines of *AtMYB2* OE transformants were grown on MS agar medium for 5 d and then transferred to nutrient medium containing 1.25 mM (high Pi), 0.0125 mM (low Pi), or 0 mM (Pi deficiency) KH_2PO_4. Seedlings were photographed 7 d after transfer. B, Quantification of primary root lengths of the seedlings depicted in A. Bars represent means ± SE of three replicates with 16 seedlings per replicate. Asterisks represent significant differences from the values of each line under the high-Pi condition ($P \leq 0.05$ from a Student's *t* test). C, Root hair development at tips of the primary root of seedlings grown in MS medium for 7 d. Bar = 1 mm. D, Quantification of root hair densities at the primary root tip of plants shown in C. Root density is the number of root hairs along 5 mm of each root above the tip. Bars represent means ± SE of three replicates with 16 seedlings per replicate. E, Quantification of lateral root numbers per plant of the seedlings depicted in A. Bars represent means ± SE of three replicates with 16 seedlings per replicate. Asterisks represent significant differences from the values of each line under the high-Pi condition ($P \leq 0.05$ from a Student's *t* test).

vector control seedlings even in high Pi (Fig. 5, A and B). Similarly, *AtMYB2* OE plants developed 5-fold more hairs near the tip of the primary root than wild-type plants even under normal Pi conditions (Fig. 5, C and D). The Pi limitation-induced reduction of primary root length and the increase in root hair density were exaggerated in *AtMYB2* OE lines, as expected. However, OE of *AtMYB2* did not exaggerate the effect of Pi limitation on lateral root development. The lateral root numbers of wild-type, vector control, and *AtMYB2* OE plants all increased by 20% to 30% in response to low Pi and Pi deficiency, respectively (Fig. 5E). Thus, OE of *AtMYB2* exaggerates some, but not all, Pi limitation-induced root architectural changes.

Taken together, these results suggested that OE of *AtMYB2* leads to a constitutive Pi starvation-induced reprogramming of root development, such as suppression of primary root growth and activation of root hair development, under Pi-sufficient conditions. Also, *AtMYB2* OE plants become more sensitive to Pi limitation than wild-type plants. These results led us to hypothesize that the inactivation of *AtMYB2* should lead to the inhibition of Pi limitation responses of roots, reduced expression of *miR399f* under Pi limitation, and reduced Pi content under Pi sufficiency or excess.

Inactivation of *AtMYB2* Does Not Affect Pi Starvation Responses

To verify the above hypothesis, we obtained an *atmyb2* mutant (SALK_045455) that contains a transfer DNA insertion in the third exon of *AtMYB2* (Supplemental Fig. S2A). This insertion mutant was designated as *atmyb2-3*. qRT-PCR analysis of *AtMYB2* expression showed that the *atmyb2-3* mutant did not produce any detectable *AtMYB2* transcript (Supplemental Fig. S2B). In low-Pi and Pi-deficient media, the inhibition of primary root growth and *miR399f* transcript levels in wild-type and *atmyb2-3* plants was comparable (Supplemental Fig. S2, C and D). Furthermore, there was no difference in the Pi

contents of roots and shoots of wild-type and *atmyb2-3* plants grown in high-Pi medium (Supplemental Fig. S2E). As the inactivation of *AtMYB2* did not produce the expected phenotypes, we concluded that there is redundancy of the function that *AtMYB2* fulfills in Pi starvation signaling.

OE of *AtMYB2* Affects the Expression of *PSI* Genes

In addition to changes in root architecture, Pi starvation also induces the expression of *PSI* genes such as the Pi transporters *AtPT1* (*Pht1;1*; Shin et al., 2004) and *AtPT2* (*Pht1;4*; Shin et al., 2004), an acid phosphatase (*AtPS2*; Baldwin et al., 2001), a glycerol-3-phosphate permease (*AtPS3*; Ramaiah et al., 2011), an S-like RNase (*AtRNS1*; Bariola et al., 1999), and a noncoding transcript (*AtIPS1*; Franco-Zorrilla et al., 2007). To test whether OE of *AtMYB2* also affects the expression of *PSI* genes, the mRNA levels of several *PSI* genes were analyzed in *AtMYB2* OE plants after transfer from normal growth medium to high-Pi, low-Pi, and Pi-deficient medium. qRT-PCR analyses showed that the expression of all *PSI* genes tested (*AtPT1*, *AtPT2*, *AtPS2*, *AtPS3*, *AtIPS1*, and *AtRNS1*) was highly induced by Pi limitation in wild-type plants (Fig. 6). In *AtMYB2* OE plants, abundance of transcripts of the phosphate transporters *AtPT1* and *AtPT2* was higher than that in wild-type plants under high-Pi and low-Pi limitation conditions but was not evident under Pi deficiency, because the expression level of the wild type was equally high (Fig. 6, A and B). These results provide some explanation of the higher Pi content of *AtMYB2* OE plants compared with the wild type under high-Pi growth (Fig. 4D). However, it is possible that other *PSI* genes, for which we did not analyze the expression patterns in this study, may also play important roles in the enhanced Pi uptake of *AtMYB2* OE plants. Expression of the acid phosphatase *AtPS2* was comparable in wild type and *AtMYB2* OE plants grown under high Pi but was induced to a greater extent in *AtMYB2* OE plants compared with the wild type under low Pi and Pi deficiency (Fig. 6C). In contrast, the abundance of *AtRNS1* and *AtIPS1* mRNA was comparable in wild-type and *AtMYB2* OE plants grown under high Pi. Although these transcripts were induced by Pi limitation in the *AtMYB2* OE plants, the magnitude of induction was less than that in wild-type plants grown under the same conditions (Fig. 6, E and F). These data indicate that *AtMYB2* is involved in the regulation of a subset of *PSI* gene expression.

AtMYB2 Directly Binds to the *miR399f* Promoter and Activates *miR399f* Expression

Two putative MYB-binding sites (MBSs; 5′-TAACTG-3′) that have opposite orientations were found by in silico analysis of the putative regulatory region of

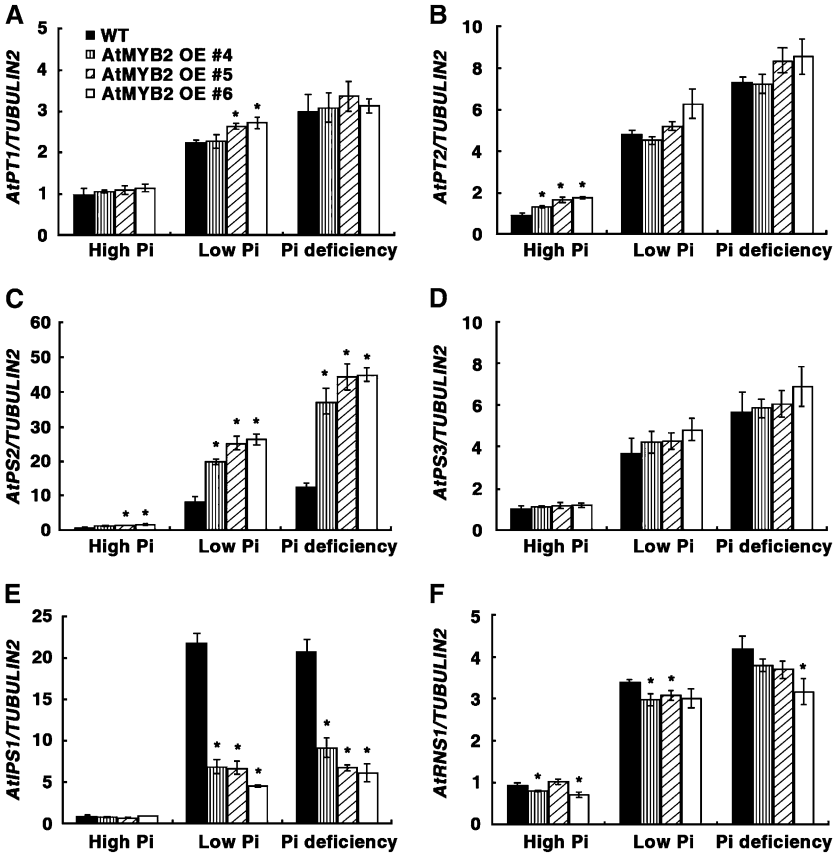

Figure 6. Expression patterns of Pi starvation-induced genes in *AtMYB2* OE plants. Seeds of the untransformed wild type (WT) and three independent lines of *AtMYB2* OE transformants were grown on MS agar medium for 7 d and then transferred to the high-Pi, low-Pi, or Pi-deficient medium described in Figure 4. Transcript levels of *AtPT1* (A), *AtPT2* (B), *AtPS2* (C), *AtPS3* (D), *AtIPS1* (E), and *AtRNS1* (F) were analyzed by qRT-PCR in total RNA extracted from the seedlings 7 d after transfer. The *TUBULIN2* transcript level was used for normalization. Bars represent means ± SD of three biological replicates with two technical replicates each. Asterisks represent significant differences from the wild type ($P \leq 0.05$ from a Student's *t* test).

miR399f (Figs. 1B and 7A). To examine whether the AtMYB2 protein binds to one or both of these MBSs, we performed electrophoretic mobility shift assays (EMSA) with ^{32}P-labeled oligonucleotides corresponding to promoter fragments containing the MBS-1 or MBS-2 motif (140 or 149 bp, respectively) and recombinant glutathione *S*-transferase (GST)-AtMYB2 or GST proteins. A GST-AtMYB2-specific mobility-retarded band indicating binding to AtMYB2 was observed with the MBS-2 oligonucleotide (Fig. 7A). The intensity of this band was enhanced by increasing the amount of GST-AtMYB2 protein in the binding reaction. No mobility-retarded bands were observed with MBS-1 oligonucleotide, indicating absence of binding.

Next, a chromatin immunoprecipitation (ChIP) assay was performed using total protein extracts of wild-type and *CaMV35S:FLAG-AtMYB2* transgenic plants. After immunoprecipitation with an antiserum against the FLAG tag, the relative contents of *miR399f* promoter fragments P1 to P4 (Fig. 7B) in the immunoprecipitates were estimated by qRT-PCR (Fig. 7C). The amplicons P1 and P2, which surrounded and included the MBS-2 region, respectively, were significantly enriched by qRT-PCR. No enrichment of the P3 amplicon that includes MBS-1, or the P4 amplicon, was observed in the *CaMV35S:FLAG-AtMYB2* extracts. Together, the results from EMSA and ChIP assays indicate that AtMYB2 directly binds to the MBS-2 region in the *miR399f* promoter in vitro and in vivo.

Next, we verified that AtMYB2 was a nucleus-localized protein. As shown in Supplemental Figure S3, the GFP signal in Arabidopsis protoplasts transiently transformed with *CaMV35S:AtMYB2-sGFP* (for synthetic GFP) was exclusively localized in the nucleus. We then tested whether *AtMYB2* can transactivate reporter gene expression from the *miR399f* promoter. Cotransformation of *atmyb2-3* protoplasts with *PromiR399f:GUS* reporter and *CaMV35S:AtMYB2-sGFP* or *CaMV35S:sGFP* (negative control) as effector construct showed that *AtMYB2-sGFP* greatly increases *miR399f* promoter activity compared with s*GFP* alone (Fig. 8). These results indicate that *AtMYB2* can function as a transcriptional activator for the *miR399f* gene in vivo.

DISCUSSION

Our results show that *AtMYB2* binds to the *miR399f* promoter, leading to the activation of *miR399f* expression. *AtMYB2* and *miR399f* are expressed in the same tissues, particularly under Pi limitation, and are also induced by Pi limitation, and they activate the same subset of *PSI* genes. Thus, we infer that AtMYB2 functions as a transcription factor regulating *miR399f*-mediated signaling in the establishment of Pi homeostasis under Pi limitation. We subsequently were able to support this role for AtMYB2 in the plant response to Pi limitation on the basis of the phenotypes of transgenic *AtMYB2* OE lines. As there were no differences with respect to phenotype in the response to Pi

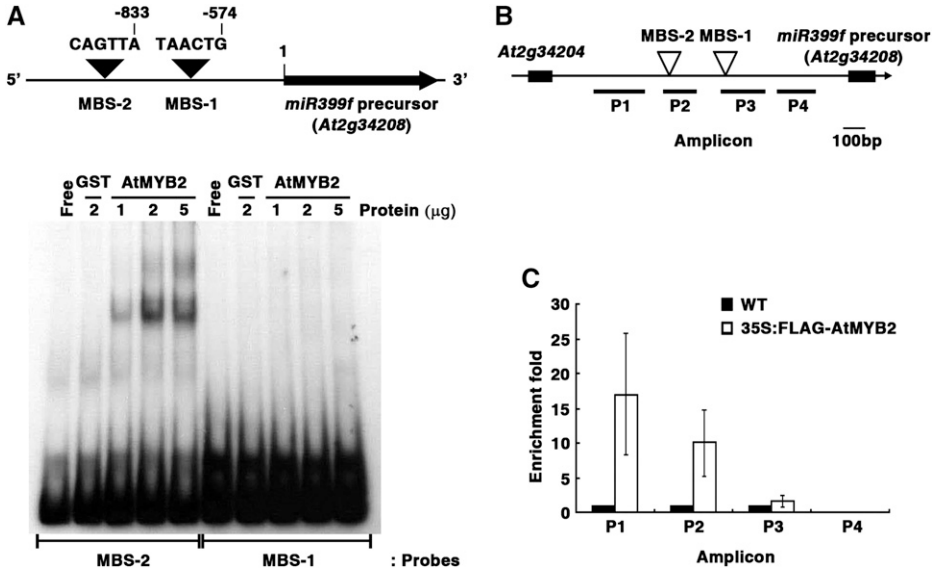

Figure 7. AtMYB2 binds to MBS-2 on the *miR399f* promoter region. A, Top, schematic representation of predicted MYB-binding sites (MBS-1 and MBS-2) in the *miR399f* promoter. Bottom, EMSA of the binding of recombinant AtMYB2 protein to oligonucleotides spanning the MBS-2 and MBS-1 regions. The autoradiogram shows resolved binding reactions of ^{32}P-labeled DNA probes (MBS-2 and MBS-1) without protein (Free) or with the indicated amounts of AtMYB2-GST (AtMYB2) or GST (negative control). B, Schematic drawing of the *miR399f* locus and locations of the ChIP assay amplicons (P1–P4). C, ChIP assay for *miR399f* chromatin regions associated with AtMYB2. The ChIP assay was performed on total protein extracts of MS-grown 3-week-old seedlings of the untransformed wild type (WT) and *CaMV35S:FLAG-AtMYB2* transformed Arabidopsis. Fold enrichment is the ratio of *CaMV35S:FLAG-AtMYB2* to wild-type signal. Bars represent means ± SD for three technical replicates.

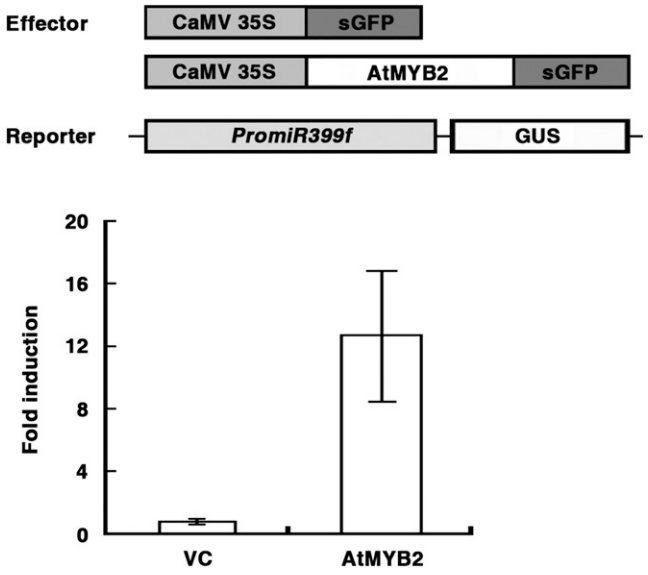

Figure 8. AtMYB2 enhances the *miR399f* promoter activity. Top, schematic representation of the effector and reporter constructs used in the transient expression assay of *miR399f* promoter activity. Each effector construct was introduced into *atmyb2-3* protoplasts along with the reporter construct and an internal control *CaMV35S*:*LUC* construct by polyethylene glycol-mediated transformation. Bottom, GUS reporter activity in each sample was obtained after normalization to LUC activity. Fold induction is the ratio of the GUS activity of *CaMV35S*:*AtMYB2-sGFP* transformed protoplasts (AtMYB2) relative to the GUS activity of *CaMV35S*:*sGFP* transformed protoplasts (vector control [VC]). Bars represent means ± SD of three technical replicates.

starvation between wild-type and null *atmyb2-3* plants (Supplemental Fig. S2), we conclude further that AtMYB2 is functionally redundant.

Our discovery of AtMYB2 as a transcription factor activating *miR399f* expression began with an in silico analysis for cis-acting elements in the 1,384-bp region upstream of the primary transcript of the *miR399f* gene (pri-*miR399f*; *At2g34208*). It has been reported that a TATA box-like sequence is located within 50 nucleotides upstream of the majority of the primary miRNA transcripts of Arabidopsis miRNA genes (Xie et al., 2005a). A TATA box-like sequence, TATAATTA, was mapped at 45 nucleotides upstream of the *miR399f* precursor (Fig. 1A), indicating that *miR399f* is a typical RNA polymerase II-transcribed independent transcription unit. In addition to the TATA box-like motif and MYB-binding sites, we found several canonical cis-regulatory elements in the *miR399f* promoter. A GNATATNC element was located at −84 bp on the *miR399f* promoter (Fig. 1B). This sequence is known to bind PHR1, a MYB transcription factor that causes upregulation of Pi-responsive genes (Rubio et al., 2001). The presence of a PHR1-binding motif in the *miR399f* promoter raises the possibility that the MYB family transcription factor PHR1 compensates at least partly for AtMYB2 function. More experiments are needed in order to both verify the role, if any, of PHR1 in the regulation of *miR399f* expression and investigate how much the two promoter-binding factors overlap or diverge in the activating capacity.

The *miR399* family in Arabidopsis consists of six members, *miR399a* to *miR399f*, all of which are induced by Pi starvation and function in Pi homeostasis by regulating the expression of *UBC24* (Fujii et al., 2005; Aung et al., 2006; Chiou et al., 2006; Doerner, 2008; Pant et al., 2008; Hsieh et al., 2009; Kuo and Chiou, 2011). We found that the putative promoter regions of *miR399a*, *miR399b*, and *miR399c* also contain GNATATNC elements (data not shown). Soybean (*Glycine max*) miRNA genes responsible for Pi starvation signaling contain several types of Pi-responsive cis-elements in their promoters, including the PHR1-binding site (Zeng et al., 2010). This suggests that the induction of several *miRNA399* family members, including *miRNA399f*, in response to Pi limitation could be mediated in part by PHR1. Defense-, hormone-, light-, and water stress-responsive cis-regulatory elements were detected in the *miR399f* promoter (Fig. 1B). This is consistent with a previous report indicating that the cis-acting elements involved in hormone and abiotic stress responses are overrepresented in miRNA promoters when compared with promoters of protein-coding genes (Megraw et al., 2006). It would be interesting to ascertain whether *miR399f* and other members of this family constitute a hub that is important for coordinating environmental cues with nutrient acquisition to modulate plant growth. It must be noted that AtMYB2, established by us as a transcriptional activator of *miR399f*, also functions in hormonal and abiotic stress signaling in Arabidopsis (Urao et al., 1996; Abe et al., 1997, 2003; Yoo et al., 2005; Guo and Gan, 2011).

Of the two MBS motifs in the *miR399f* promoter, only MBS-2, the more distal element in the pri-*miR399f* sequence, was identified as a functional binding site for the AtMYB2 transcription factor in vitro and in vivo (Fig. 7). This suggests that both the core element sequences and the flanking sequences are important for efficient binding of AtMYB2 on the *miR399f* promoter. MBS motifs are found in the promoters of many *miR399* family members of Arabidopsis and rice (data not shown). From an analysis of 1.5-kb upstream sequences of *miR399a*, *miR399b*, *miR399c*, *miR399d*, and *miR399e*, we found that *miR399b* and *miR399c* have MBS motifs in their promoter regions (Supplemental Table S2). However, in contrast to *miR399f*, transcript levels of *miR399b* and *miR399c* genes in *AtMYB2* OE plants were comparable to those in wild-type plants (Supplemental Fig. S4). These in silico promoter analyses and subsequent gene expression analyses suggest that the transcriptional regulation by *AtMYB2* affects specifically the *miRNA399f* gene among the *miR399* family members. The upstream region of other Pi-responsive miRNA genes, including *miR156a*, *miR156e*, and *miR2111a*, also contain MBS motifs (Supplemental Table S2). Additional experimental data will be required to ascertain whether *AtMYB2* is also involved in the regulation of *miR156a*, *miR156e*, and *miR2111a* expression in

response to Pi starvation or whether this group of miRNAs diversifies into additional functions. Further analyses of promoters of the miRNA genes that regulate low-Pi responses should illuminate other mechanisms and the signaling cross talk that govern their expression.

MATERIALS AND METHODS

Plant Materials and Stress Treatments

All Arabidopsis (*Arabidopsis thaliana*) lines were in the ecotype Columbia-0 background. The *atmyb2-3* mutant (SALK_045455) was obtained from the Arabidopsis Biological Resource Center at Ohio State University (http://www.arabidopsis.org/). Transgenic lines were generated by *Agrobacterium tumefaciens*-mediated transformation using the floral dip method as described (Clough and Bent 1998). Homozygous lines were generated by back-crossing and were used in the experiments. The genotype of the transformants was verified by PCR. Seeds were germinated and grown on MS medium containing 1% Suc and 0.7% (or 1.2%) agar, pH 5.7. For testing the effect of Pi limitation, 5- or 7-d-old seedlings were transferred to growth medium containing 1% Suc, 1/20× micronutrients (Miura et al., 2005), and 1.25 mM KH_2PO_4 (high Pi; this is equivalent to the Pi content of 1× MS), 0.0125 mM KH_2PO_4 (low Pi), or 0 mM KH_2PO_4 (Pi deficiency) for the indicated times (Miura et al., 2005). Plants were grown in a growth chamber at 22°C under a 16-h-light/8-h-dark cycle.

qRT-PCR Analysis

Total RNA was isolated using an RNeasy Kit (Qiagen) according to the manufacturer's instructions and treated with DNase I (Promega) to remove genomic DNA contamination. Total RNA (2 μg) was used for first-strand complementary DNA (cDNA) synthesis using a cDNA Synthesis Kit (Invitrogen) and subjected to qRT-PCR analysis. The primers used in qRT-PCR analysis are described in Supplemental Table S1. The SsoFast EvaGreen Supermix (Bio-Rad) was used for the PCRs. PCR conditions were 50°C for 2 min, 95°C for 10 min, and 40 cycles of 95°C for 15 s and 60°C for 60 s. The relative expression levels of all the samples were automatically calculated and analyzed three times using CFX Manager software (Bio-Rad).

Northern-Blot Analysis of miRNAs

Northern-blot analysis of miRNAs was performed essentially as described (Xie et al., 2005b). Total RNA was extracted from seedlings using Plant RNA reagent (Invitrogen) following the supplier's instructions. Briefly, total RNA (20 μg) was resolved on a 15% polyacrylamide gel containing 7 M urea and transferred to an Amersham Hybrid-N^+ membrane (GE Healthcare). The probe complementary to *miR399f* (5′-UGCCAAAGGAGAUUUGCCCGG-3′) was 5′-end labeled with [γ-^{32}P]ATP using Optikinase (Affymetrix/USB). Blots were prehybridized for at least 1 h and hybridized for 24 h in PerfectHyb Plus Hybridization buffer (Sigma) at 37°C. Posthybridization, blots were washed successively at 42°C with 2× SSC and 0.1% SDS for 15 min, 0.5× SSC and 0.1% SDS for 15 min, and 0.1× SSC and 0.1% SDS for 15 min.

Pi Measurement

Total Pi contents were analyzed as described previously (Fujii et al., 2005).

Expression and Purification of Recombinant GST-AtMYB2 Protein

AtMYB2 cDNA was inserted as a *Bam*HI/*Sal*I fragment into the same sites of *pGEX-2T* (Amersham Biosciences) to create an in-frame GST fusion. The primers used in cDNA cloning are described in Supplemental Table S1. The construct was verified by sequencing. *pGEX-2T*::*AtMYB2* was introduced into *Escherichia coli* strain BL21 (Merck). For protein expression, cells were induced for 3 h at 30°C with 0.5 mM isopropylthio-β-galactoside. Induced cells were harvested, suspended in 1× GST bind/wash buffer (4.3 mM Na_2HPO_4, 1.47 mM KH_2PO_4, 137 mM NaCl, and 2.7 mM KCl, pH 7.3), incubated on ice for 20 min, and lysed by sonication. After centrifugation at 12,000 rpm at 4°C for 30 min, the supernatant was added to 0.5 mL of Glutathione-Agarose 4B (PEPTRON) that had been equilibrated with 1× GST bind/wash buffer. The slurry was mixed gently by shaking at room temperature for 30 min. The resin was then collected and washed two or three times with 10 mL of 1× GST bind/wash buffer. GST-AtMYB2 was eluted in 1 mL of 1× GST elution buffer (50 mM Tris-HCl, pH 8.0, and 10 mM reduced glutathione).

EMSA

To generate the ^{32}P-labeled DNA probes, oligonucleotides spanning the MYB-binding sites on the *miR399f* promoter, MBS-1 (140 bp) and MBS-2 (149 bp), were annealed and the 5′ overhangs were filled in using the Klenow fragment of DNA polymerase (Takara), dCTP, dGTP, dTTP, and [α-^{32}P]dATP. The DNA-binding reaction was allowed to proceed at 25°C for 20 min in binding buffer (20 mM HEPES, pH 7.9, 0.5 mM dithiothreitol, and 0.1 mM EDTA), 50 mM KCl, 15% glycerol, 1 μg of poly(dI-dC), and various concentrations of purified bacterially expressed AtMYB2 protein. The reaction was started by adding ^{32}P-labeled DNA probe (40,000 cpm) and allowed to proceed at 25°C for 30 min. The reaction mixture was then subjected to electrophoresis on an 8% polyacrylamide gel in 0.5× Tris-borate/EDTA buffer at 80 V for 3 h. The gel was dried, mounted for autoradiography with intensifying screens, and exposed at −70°C.

ChIP Assay

The Gateway system was used to generate a *CaMV35S*:*FLAG-AtMYB2* construct in the *pGWB12* vector. This construct expresses FLAG-tagged full-length AtMYB2 protein. The construct was introduced into wild-type Arabidopsis plants through *A. tumefaciens*-mediated (strain *GV3101*) transformation. ChIP assays were performed as described by Saleh et al. (2008) using leaf tissue (100 mg) from 3-week-old plants. Monoclonal anti-FLAG M2 (Sigma) was used for immunoprecipitation. The amount of immunoprecipitated DNA was quantified by qRT-PCR. The primers used in the ChIP assay are listed in Supplemental Table S1.

Measurement of Promoter Activity

Transcriptional activity of the *miR399f* promoter was analyzed in Arabidopsis protoplasts as described by Zhu et al. (2008). The reporter construct was *PromiR399f*:*GUS*, and the effector constructs were *CaMV35S*:*AtMYB2*-s*GFP* and *CaMV35S*:s*GFP*. Plasmids carrying the reporter and an effector gene construct, along with an internal control plasmid carrying a *CaMV35*:*LUC* gene construct, were introduced into protoplasts prepared from leaves of 20-d-old *atmyb2-3* plants by polyethylene glycol-mediated transformation as described by Baek et al. (2004). Fluorescence was measured using a SpectraMax GEMINI XPS spectrofluorometer (Molecular Devices) using the SoftMax Pro 5 software. GUS activity was normalized to luciferase activity to eliminate experimental variation between samples.

Histochemical Analysis of GUS Activity

Plants expressing the *PromiR399f*:*GUS* or *ProAtMYB2*:*GUS* transgenes in the wild-type background were used for histological analysis. Seedlings of transgenic plants grown in various levels of Pi were incubated at 30°C for 6 h in the dark in staining buffer (0.5 M Tris, pH 7.0, and 10% Triton X-100) containing 1 mM 5-bromo-4-chloro-3-indolyl-β-D-glucuronide. Chlorophyll was removed with an ethanol series consisting of 20%, 35%, 50%, and 70% ethanol washes at room temperature for 30 min each.

Supplemental Data

The following materials are available in the online version of this article.

Supplemental Figure S1. Chlorosis phenotype in *AtMYB2* OE plants.

Supplemental Figure S2. Responses of *atmyb2-3* to Pi starvation.

Supplemental Figure S3. Subcellular localization of AtMYB2.

Supplemental Figure S4. Expression patterns of *miR399b* and *miR399c* in *AtMYB2* OE plants.

Supplemental Table S1. List of primers used in this study.

Supplemental Table S2. MBS elements in a Pi-responsive miRNA promoter.

Supplemental Materials and Methods S1.

ACKNOWLEDGMENTS

We thank the Arabidopsis Biological Resource Center for providing mutant seeds.

Received August 20, 2012; accepted November 12, 2012; published November 15, 2012.

LITERATURE CITED

Abe H, Urao T, Ito T, Seki M, Shinozaki K, Yamaguchi-Shinozaki K (2003) *Arabidopsis* AtMYC2 (bHLH) and AtMYB2 (MYB) function as transcriptional activators in abscisic acid signaling. Plant Cell **15:** 63–78

Abe H, Yamaguchi-Shinozaki K, Urao T, Iwasaki T, Hosokawa D, Shinozaki K (1997) Role of *Arabidopsis* MYC and MYB homologs in drought- and abscisic acid-regulated gene expression. Plant Cell **9:** 1859–1868

Aung K, Lin SI, Wu CC, Huang YT, Su CL, Chiou TJ (2006) *pho2*, a phosphate overaccumulator, is caused by a nonsense mutation in a microRNA399 target gene. Plant Physiol **141:** 1000–1011

Baek D, Nam J, Koo YD, Kim DH, Lee J, Jeong JC, Kwak SS, Chung WS, Lim CO, Bahk JD, et al (2004) Bax-induced cell death of *Arabidopsis* is meditated through reactive oxygen-dependent and -independent processes. Plant Mol Biol **56:** 15–27

Baldwin JC, Karthikeyan AS, Raghothama KG (2001) LEPS2, a phosphorus starvation-induced novel acid phosphatase from tomato. Plant Physiol **125:** 728–737

Bari R, Pant BD, Stitt M, Scheible WR (2006) PHO2, microRNA399, and PHR1 define a phosphate-signaling pathway in plants. Plant Physiol **141:** 988–999

Bariola PA, MacIntosh GC, Green PJ (1999) Regulation of S-like ribonuclease levels in Arabidopsis: antisense inhibition of RNS1 or RNS2 elevates anthocyanin accumulation. Plant Physiol **119:** 331–342

Bonnet E, Van de Peer Y, Rouzé P (2006) The small RNA world of plants. New Phytol **171:** 451–468

Chen ZH, Nimmo GA, Jenkins GI, Nimmo HG (2007) BHLH32 modulates several biochemical and morphological processes that respond to Pi starvation in *Arabidopsis*. Biochem J **405:** 191–198

Chiou TJ, Aung K, Lin SI, Wu CC, Chiang SF, Su CL (2006) Regulation of phosphate homeostasis by microRNA in *Arabidopsis*. Plant Cell **18:** 412–421

Clough SJ, Bent AF (1998) Floral dip: a simplified method for *Agrobacterium*-mediated transformation of *Arabidopsis thaliana*. Plant J **16:** 735–743

Desnos T (2008) Root branching responses to phosphate and nitrate. Curr Opin Plant Biol **11:** 82–87

Devaiah BN, Karthikeyan AS, Raghothama KG (2007a) WRKY75 transcription factor is a modulator of phosphate acquisition and root development in Arabidopsis. Plant Physiol **143:** 1789–1801

Devaiah BN, Madhuvanthi R, Karthikeyan AS, Raghothama KG (2009) Phosphate starvation responses and gibberellic acid biosynthesis are regulated by the MYB62 transcription factor in *Arabidopsis*. Mol Plant **2:** 43–58

Devaiah BN, Nagarajan VK, Raghothama KG (2007b) Phosphate homeostasis and root development in Arabidopsis are synchronized by the zinc finger transcription factor ZAT6. Plant Physiol **145:** 147–159

Doerner P (2008) Phosphate starvation signaling: a threesome controls systemic P(i) homeostasis. Curr Opin Plant Biol **11:** 536–540

Franco-Zorrilla JM, Valli A, Todesco M, Mateos I, Puga MI, Rubio-Somoza I, Leyva A, Weigel D, García JA, Paz-Ares J (2007) Target mimicry provides a new mechanism for regulation of microRNA activity. Nat Genet **39:** 1033–1037

Fujii H, Chiou TJ, Lin SI, Aung K, Zhu JK (2005) A miRNA involved in phosphate-starvation response in *Arabidopsis*. Curr Biol **15:** 2038–2043

Guo Y, Gan S (2011) AtMYB2 regulates whole plant senescence by inhibiting cytokinin-mediated branching at late stages of development in Arabidopsis. Plant Physiol **156:** 1612–1619

Hillwig MS, Lebrasseur ND, Green PJ, Macintosh GC (2008) Impact of transcriptional, ABA-dependent, and ABA-independent pathways on wounding regulation of RNS1 expression. Mol Genet Genomics **280:** 249–261

Hinsinger P (2001) Bioavailability of soil inorganic P in the rhizosphere as affected by root-induced chemical changes: a review. Plant Soil **237:** 173–195

Hsieh LC, Lin SI, Shih AC, Chen JW, Lin WY, Tseng CY, Li WH, Chiou TJ (2009) Uncovering small RNA-mediated responses to phosphate deficiency in Arabidopsis by deep sequencing. Plant Physiol **151:** 2120–2132

Jones-Rhoades MW, Bartel DP (2004) Computational identification of plant microRNAs and their targets, including a stress-induced miRNA. Mol Cell **14:** 787–799

Jones-Rhoades MW, Bartel DP, Bartel B (2006) MicroRNAS and their regulatory roles in plants. Annu Rev Plant Biol **57:** 19–53

Kuo HF, Chiou TJ (2011) The role of microRNAs in phosphorus deficiency signaling. Plant Physiol **156:** 1016–1024

Lei M, Zhu C, Liu Y, Karthikeyan AS, Bressan RA, Raghothama KG, Liu D (2011) Ethylene signalling is involved in regulation of phosphate starvation-induced gene expression and production of acid phosphatases and anthocyanin in *Arabidopsis*. New Phytol **189:** 1084–1095

Li Z, Gao Q, Liu Y, He C, Zhang X, Zhang J (2011) Overexpression of transcription factor ZmPTF1 improves low phosphate tolerance of maize by regulating carbon metabolism and root growth. Planta **233:** 1129–1143

Liang G, Yang F, Yu D (2010) MicroRNA395 mediates regulation of sulfate accumulation and allocation in *Arabidopsis thaliana*. Plant J **62:** 1046–1057

Mallory AC, Vaucheret H (2006) Functions of microRNAs and related small RNAs in plants. Nat Genet (Suppl) **38:** S31–S36

Megraw M, Baev V, Rusinov V, Jensen ST, Kalantidis K, Hatzigeorgiou AG (2006) MicroRNA promoter element discovery in *Arabidopsis*. RNA **12:** 1612–1619

Miura K, Rus A, Sharkhuu A, Yokoi S, Karthikeyan AS, Raghothama KG, Baek D, Koo YD, Jin JB, Bressan RA, et al (2005) The *Arabidopsis* SUMO E3 ligase SIZ1 controls phosphate deficiency responses. Proc Natl Acad Sci USA **102:** 7760–7765

Osmont KS, Sibout R, Hardtke CS (2007) Hidden branches: developments in root system architecture. Annu Rev Plant Biol **58:** 93–113

Pant BD, Buhtz A, Kehr J, Scheible WR (2008) MicroRNA399 is a long-distance signal for the regulation of plant phosphate homeostasis. Plant J **53:** 731–738

Pant BD, Musialak-Lange M, Nuc P, May P, Buhtz A, Kehr J, Walther D, Scheible WR (2009) Identification of nutrient-responsive Arabidopsis and rapeseed microRNAs by comprehensive real-time polymerase chain reaction profiling and small RNA sequencing. Plant Physiol **150:** 1541–1555

Péret B, Clément M, Nussaume L, Desnos T (2011) Root developmental adaptation to phosphate starvation: better safe than sorry. Trends Plant Sci **16:** 442–450

Poirier Y, Bucher M (2002) Phosphate transport and homeostasis in *Arabidopsis*. The Arabidopsis Book **1**: e0024, doi/10.1199/tab.0024

Raghothama KG (1999) Phosphate acquisition. Annu Rev Plant Physiol Plant Mol Biol **50:** 665–693

Ramaiah M, Jain A, Baldwin JC, Karthikeyan AS, Raghothama KG (2011) Characterization of the phosphate starvation-induced glycerol-3-phosphate permease gene family in Arabidopsis. Plant Physiol **157:** 279–291

Rouached H, Arpat AB, Poirier Y (2010) Regulation of phosphate starvation responses in plants: signaling players and cross-talks. Mol Plant **3:** 288–299

Rubio V, Linhares F, Solano R, Martín AC, Iglesias J, Leyva A, Paz-Ares J (2001) A conserved MYB transcription factor involved in phosphate starvation signaling both in vascular plants and in unicellular algae. Genes Dev **15:** 2122–2133

Saleh A, Alvarez-Venegas R, Avramova Z (2008) An efficient chromatin immunoprecipitation (ChIP) protocol for studying histone modifications in *Arabidopsis* plants. Nat Protoc **3:** 1018–1025

Shin H, Shin HS, Dewbre GR, Harrison MJ (2004) Phosphate transport in *Arabidopsis*: Pht1;1 and Pht1;4 play a major role in phosphate acquisition from both low- and high-phosphate environments. Plant J **39:** 629–642

Sunkar R, Li YF, Jagadeeswaran G (2012) Functions of microRNAs in plant stress responses. Trends Plant Sci **17:** 196–203

Urao T, Noji M, Yamaguchi-Shinozaki K, Shinozaki K (1996) A transcriptional activation domain of ATMYB2, a drought-inducible *Arabidopsis* Myb-related protein. Plant J **10:** 1145–1148

Xie Z, Allen E, Fahlgren N, Calamar A, Givan SA, Carrington JC (2005a) Expression of Arabidopsis *MIRNA* genes. Plant Physiol **138:** 2145–2154

Xie Z, Allen E, Wilken A, Carrington JC (2005b) DICER-LIKE 4 functions in trans-acting small interfering RNA biogenesis and vegetative phase change in *Arabidopsis thaliana*. Proc Natl Acad Sci USA **102:** 12984–12989

Yamasaki H, Abdel-Ghany SE, Cohu CM, Kobayashi Y, Shikanai T, Pilon M (2007) Regulation of copper homeostasis by micro-RNA in *Arabidopsis*. J Biol Chem **282:** 16369–16378

Yi K, Wu Z, Zhou J, Du L, Guo L, Wu Y, Wu P (2005) OsPTF1, a novel transcription factor involved in tolerance to phosphate starvation in rice. Plant Physiol **138:** 2087–2096

Yoo JH, Park CY, Kim JC, Heo WD, Cheong MS, Park HC, Kim MC, Moon BC, Choi MS, Kang YH, et al (2005) Direct interaction of a divergent CaM isoform and the transcription factor, MYB2, enhances salt tolerance in *Arabidopsis*. J Biol Chem **280:** 3697–3706

Yuan H, Liu D (2008) Signaling components involved in plant responses to phosphate starvation. J Integr Plant Biol **50:** 849–859

Zeng HQ, Zhu YY, Huang SQ, Yang ZM (2010) Analysis of phosphorus-deficient responsive miRNAs and *cis*-elements from soybean (*Glycine max* L.). J Plant Physiol **167:** 1289–1297

Zhu J, Jeong JC, Zhu Y, Sokolchik I, Miyazaki S, Zhu JK, Hasegawa PM, Bohnert HJ, Shi H, Yun DJ, et al (2008) Involvement of *Arabidopsis* HOS15 in histone deacetylation and cold tolerance. Proc Natl Acad Sci USA **105:** 4945–4950